Spatio-temporal distribution and chemical composition of PM$_{2.5}$ in Changsha, China

Nan-Nan Zhang[1,2,3] · Yang Guan[3] · Lei Yu[3] · Fang Ma[1,2] · Yi-Fan Li[1,2]

Abstract

The rapid economic development and significant expansion of urban agglomerations in China have resulted in issues associated with haze and photochemical smog. Central China, a transitional zone connecting the eastern coast and western interior, suffers from increasing atmospheric pollution. This study performed a spatio-temporal analysis of fine particulate matter (PM$_{2.5}$) pollution in Changsha, a provincial capital located in central China. Samples of PM$_{2.5}$ were collected at five different functional areas from September 2013 to August 2014. The PM$_{2.5}$ concentration at the five sampling sites was the highest in winter and the lowest in summer, with an average annual PM$_{2.5}$ concentration of 105.2 ± 11.0 μg/m^3. On average, residential sites had the highest concentrations of PM$_{2.5}$ while suburban sites had the lowest. We found that inorganic ionic species were dominant (~48%), organic species occupied approximately 25%, whereas EC (~3.7%) contributed insignificantly to the total PM$_{2.5}$ mass. Ion balance calculations show that the PM$_{2.5}$ samples at all sites were acidic, with increased acidity in spring and summer compared with autumn and winter. Air quality in Changsha is controlled by four major air masses: (1) Wuhan and the surrounding urban clusters, (2) the Changsha-Zhuzhou-Xiangtan urban agglomeration and the surrounding cities, and (3) southern and (4) eastern directions. The north–south transport channel is the most significant air mass trajectory in Changsha and has a significant impact on PM$_{2.5}$ pollution.

Keywords PM$_{2.5}$ · Aerosol components · Spatio-temporal distribution · Source apportionment · Yangtze River Economic Belt

✉ Yi-Fan Li
ijrc_pts_paper@yahoo.com

1 International Joint Research Center (IJRC-PTS), State Key Laboratory of Urban Water Resource and Environment, Harbin Institute of Technology, Harbin 150090, China

2 School of Environment, Harbin Institute of Technology, Harbin 150090, China

3 Chinese Academy of Environmental Planning, and, Beijing 100012, China

1 Introduction

In recent decades, China has suffered from extremely severe and persistent haze events, within which there is a significant contribution of fine particulate matter ($PM_{2.5}$) (Qiu et al. 2016; Shi et al. 2017a, 2017b; Yan et al. 2018; Zhang et al. 2018a). To curb $PM_{2.5}$ pollution in China, the Ambient Air Quality Standards (AAQS; GB 3095–2012) were updated in 2012, which include the regulation of $PM_{2.5}$ as a crucial pollutant (Zheng et al. 2016; Ma et al. 2017; Zhang et al. 2017a, 2017b). Compared with inhalable particles (PM_{10}) or total suspended particulate (TSP), $PM_{2.5}$ has a small particle size, a longer residence time, a long transport distance and a more significant impact on human health and air quality (Charlson et al. 1992; Haywood and Ramaswamy 1998). Numerous epidemiological and toxicological studies found that 3.45 million premature deaths worldwide were related to $PM_{2.5}$ pollution in 2007 (Zhang et al. 2017a, 2017b). Guan et al. (2019) indicated that the overall premature mortality attributed to $PM_{2.5}$ exposure in China was as high as 820 thousand cases in 2017.

Previous studies have indicated that the chemical composition of $PM_{2.5}$ is closely associated with regional urban development, seasonal changes, and geographic factors. Zíková et al. (2016) reported that mobile sources have a greater impact on economically developed cities, such as Beijing, while NO_3^-, which is related to motor vehicle emissions, is a secondary ion with strong cumulative effects that have high rates of contribution during heavy pollution. Wang et al. (2002) found that the proportion of WSIs in Nanjing $PM_{2.5}$ was much higher than that in PM_{10} and was sufficiently acidic to cause increased harm to humans and buildings. Seasonal changes also affect the WSI content. For example, NO_3^- and SO_4^{2-} have clear seasonal changes and similar trends in the Beijing-Tianjin-Hebei (BTH) regions. Coal-burning and motor vehicle emissions in winter are the principal reasons for the increases in NO_3^- and SO_4^{2-} concentrations (Zíková et al. 2016). The concentrations of NO_3^-, SO_4^{2-}, and NH_4^+ in $PM_{2.5}$ throughout the suburbs of Shanghai were lower in the summer than in the winter, whereas Ca^{2+}, K^+, and Mg^{2+} concentrations were higher in summer (Wang et al. 2016a). Wang et al. (2012) showed that contributions from Ca^{2+} and Mg^{2+} were higher in the spring and summer, which they suggested is related to the impacts that sandstorms, in northern China, have on the movement of $PM_{2.5}$ in Shanghai. The seasonal variations in the NO_3^- concentration in Suzhou and Hangzhou in the Yangtze River Delta (YRD) were consistent with the variations in Chongqing but different from those in Tianjin (Wang et al. 2015). Secondary pollution at Tianjin was the main reason for higher concentrations of NO_3^- in the summer and lower concentrations in the winter. Therefore, based on these studies, we note that water-soluble ionic components are similar among the same urban agglomerations but significantly different among different urban agglomerations.

In recent years, numerous field measurements have been performed in China to characterize $PM_{2.5}$ pollution and its chemical composition. These studies mostly focused on BTH, YRD, Pearl River Delta (PRD), and other economically developed or densely populated areas (Wang et al. 2016b; Chen et al. 2017; Zhang et al. 2018b). Very few studies have considered urban agglomerations in the middle reaches of the Yangtze River, despite the implementation of development strategies in central China and the associated rapid economic growth and industrialization over previous decades. This has resulted in a significant increase in the anthropogenic emissions in the Yangtze River Economic Belt. Thus, the Changsha-Zhuzhou-Xiangtan (CZX) region was included as one of the key areas for China's national air pollution control program within the 12th Five-Year Plan on Air Pollution Prevention and Control in Key Regions (MEP 2012).

In recent years, Changsha has rapidly developed and industrialized. As the central core city of the Yangtze River Economic Belt, as well as the provincial capital of Hunan Province, it is also a relocation site for a large number of industries transitioning from the YRD and PRD (Zhang et al. 2018c). However, relevant studies on the pollution in this area are rare. Studies on the relationships between the $PM_{2.5}$ mass concentration and its chemical components in cities and suburban areas in central China are particularly inadequate. The objectives of this study were to investigate the spatio-temporal variations of the major chemical components in $PM_{2.5}$ surrounding Changsha and discover the potential sources and transportation processes. Our results highlight the major determinants of the chemical components in $PM_{2.5}$ aerosols and offer scientific support for the development of effective regional air quality improvement strategies for central China.

2 Materials and methods

2.1 Site description and sampling procedure

In order to explore the spatial distribution of air pollution in Changsha, sampling sites were carefully chosen to reflect this spatial variation, sampling areas ($n = 5$) consisted of two residential sites, one roadside site surrounded by two main roads, one industrial site, and one suburban site. The locating and detailed information of the sampling sites were shown in Table 1 and Fig. 1. The instruments used in this study were installed on the proofs of the buildings with the height of about 10–30 m above the ground level.

Daily aerosol $PM_{2.5}$ samples were collected from September 2013 to August 2014 by employing a four-Channel sampler (TH-16A, Tianhong Instrument Co., China) equipped with a 90 mm filter at a flow rate of 16.7 L·min^{-1}. The filters were changed every 22 h (from 10:00 a.m. to 8:00 a.m. the next day). A quartz and PTFE filters were placed on the sampler. The samples collected from quartz filters were used for OC, EC, and WSI analysis while the samples collected from the PTFE filter were used for metal element analysis. Field blank filters were also collected without ambient air passing through the instrument during the sampling periods. In total, 1605 $PM_{2.5}$ samples were collected during the following periods: September 2 to October 18, 2013 (autumn, 405 samples), December 4, 2013 to January 14, 2014 (winter,

Table 1 Functional designations and locations of the monitoring sites

Sampling site	Functional area	Location	Coordinate	Height
Wangcheng (WC)	Residential	The Hunan University of Chinese Medicine campus	28.13ºN, 112.89°E	30 m
Yuhua (YH)	Residential	Southern Changsha (downwind from Changsha in winter), surrounded by residential and light commercial areas	28.12ºN, 113.03°E	25 m
Furong (FR)	Roadside	Changsha Railway Station (surrounded by two main roads)	28.20ºN, 113.01°E	10 m
Changsha (CS)	Industrial	Industrial district, consisting mainly of light industries (e.g., machine production, paint production, and food and beverage preparation)	28.24ºN, 113.14°E	20 m
Shaping (SP)	Suburban	Control site (background particulate pollution)	28.33ºN, 113.07°E	15 m
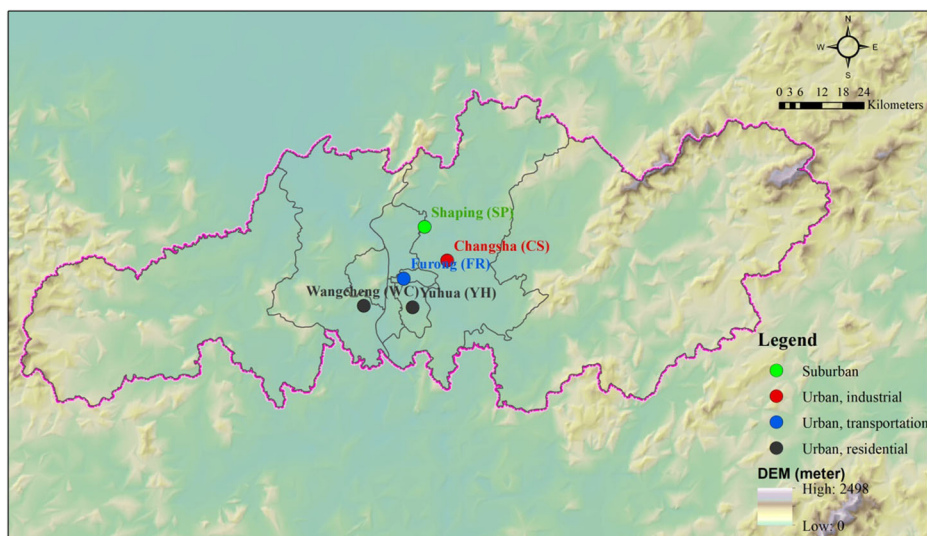
Fig. 1 Map indicating the location of each monitoring site

420 samples), March 30 to May 28, 2014 (spring, 285 samples), and June 3 to August 29, 2014 (summer, 495 samples).

The sampler was calibrated with a flow meter before and after sampling. An X-ray instrument was used to check the filters for defects, such as sand holes. The quartz filter was pre-combusted for 5 h at 500 °C and then stored in a controlled room (25 °C and 40% relative humidity, RH) for 48 h prior to sampling. After sampling, the samples and blank filters were stored at −15 °C to prevent the evaporation of volatile components before analysis.

2.2 Analytical methods

$PM_{2.5}$ mass concentrations were determined gravimetrically and each sample was weighed twice using an electronic balance (AX105DR Mettler-Toledo Ltd., Switzerland) with a sensitivity of 0.01 mg.

An area of 2.0 cm^2 of each filter, including a blank sample, was cut to analyze elements. Firstly, the MWS-3+ Microwave Digestion System (Berghof, Germany) was used for sample pretreatment following metal extraction from the filter material using the method developed by the United States Environmental Protection Agency (US EPA; Compendium Method IO-3.1). The US EPA has defined this method as a standard for the extraction of metallic elements (EPA Method-3051). Subsequently, inductively coupled plasma-mass spectrometry (ICP-MS) was used to determine the concentrations of the elements. The major elements include Na, Mg, K, Ca, Al, V, Cr, Mn, Fe, Co, Ni, Cu, Zn, As, Cs, Ag, Cd, P, Ti, and Pb. The method detection limit (MDL) of the elements ranged from 0.1 to 1 ng m^{-3}, and the uncertainties were < 5%.

A small portion of each filter (area of 2.0 cm^2) was cut to analyze the water-soluble ions. The filters were placed into approximately 50 mL of ultrapure water (18.2 MΩ·cm, 25 °C) in a 100 mL PTFE volumetric flask. The flask, containing the sample, was sonicated for 30 min in an ultrasonic bath. The extracted solution was then filtered through a 0.45 μm PTFE filter (Gelman Sciences Inc., USA) and subsequently used for WSI and low-weight organic acid analysis. Two ion chromatographs (ICS-2000 for cations and ICS 2500 for anions, Dionex

Corp.) were used to measure the WSI content in the extracted solution. Five cations (i.e., Na^+, K^+, NH_4^+, Ca^{2+}, and Mg^{2+}), four anions (i.e., SO_4^{2-}, NO_3^-, Cl^-, and F^-), and three low-weight organic acid ions (formate, acetate, and oxalate) were measured based on the procedures reported in Guo et al. (2009). The detection limits for SO_4^{2-}, NO_3^-, Cl^-, F^-, NH_4^+, Na^+, K^+, Ca^{2+}, and Mg^{2+} were 0.030, 0.027, 0.012, 0.010, 0.020, 0.025, 0.019, 0.037, and 0.020 $\mu g \cdot m^{-3}$, respectively.

A 0.5 cm^2 punch area from each filter was analyzed using a thermal/optical reflectance carbon analyzer from the Desert Research Institute (Model 2001, DRI, USA), following the IMPROVE thermal/optical reflectance protocol (Huang et al. 2014). The OC is defined as $OC1 + OC2 + OC3 + OC4 + OPC$, whereas EC is defined as $EC1 + EC2 + EC3 - OPC$ (Watson et al. 2005). Based on previous studies, organic matter (OM) is calculated as $OM = 1.6 \times OC$, where 1.6 is the conversion factor (White and Roberts 1997; Lim and Turpin 2002; Chow et al. 2002). Due to the catalytic oxidation-reduction reactions and other processes in the system, a sucrose solution was used before every experiment to calibrate the instrument. To determine the carbon background, we analyzed each sample filter alongside three blank filters, each following identical procedures, and used the mean value of the three blank experiments as the carbon background value.

2.3 Back trajectory analysis

To investigate the origins and transport pathways of the air masses arriving at the sampling sites, a back-trajectory simulation was performed with the NOAA/ARL Hybrid Single-Particle Lagrangian Integrated Trajectory (HYSPLIT) model (Draxler and Hess 1998). The model conducted 48-h back trajectories every 4 h, starting at 4:00, 8:00, 12:00, and 20:00, at a 100-m height above the central point of Changsha (28.21°N, 112.96°E). The meteorological data used for the HYSPLIT simulations derive from the GDAS (Global Data Assimilation System) of the NCEP (National Centers for Environmental Prediction).

3 Results and discussion

3.1 Frequency distribution of $PM_{2.5}$ concentrations

The daily concentrations of $PM_{2.5}$ at all sites ranged from 22.9 to 259.9 $\mu g/m^3$, with an annual mean concentration of 105.2 ± 11.0 $\mu g/m^3$. For the five sampling sites, the mean $PM_{2.5}$ concentration was 111.6 ± 54.4 $\mu g/m^3$ (FR), 105.5 ± 45.7 $\mu g/m^3$ (CS), 90.4 ± 39.4 $\mu g/m^3$ (SP), 105.7 ± 48.0 $\mu g/m^3$ (WC), and 118.8 ± 47.9 $\mu g/m^3$ (YH). The SPSS 13.3 software was used to analyze statistically significant relationships in the average daily $PM_{2.5}$ concentration data (Fig. 2). The average daily concentrations during the sampling period did not follow a normal distribution but showed a generally near-normal distribution. Approximately 74.8% of the daily concentrations exceeded the national secondary standards stipulated in the AAQS (GB 3095–2012, 35 $\mu g/m^3$) and 23.3% of the days were characterized as 'severe' or 'worse' pollution. For the five sites, 80.8% (YH), 70.3% (WC), 60.8% (SP), 64.6% (CS), and 70.1% (FR) of the days exceeded the $PM_{2.5}$ concentration of 35 $\mu g/m^3$.

For comparability, this study used $PM_{2.5}$ concentration ground monitoring data for Chinese cities released by the Ministry of Environmental Protection of China (MEP). From 2013 to 2017, Changsha's annual $PM_{2.5}$ concentrations were 83.0, 74.0, 61.0, 53.0, and 52.0 $\mu g/m^3$,
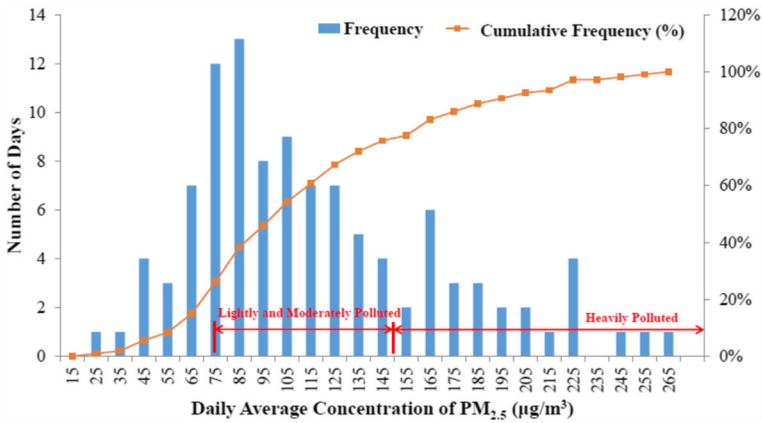
Fig. 2 Frequency distribution of the average daily PM$_{2.5}$ concentrations during the sampling period

respectively, showing a sharp decline in accordance with China's comprehensive implementation of the Air Pollution Prevention Action Plan (Zhang and Wu 2018). However, PM$_{2.5}$ concentrations in Changsha remained consistently higher than 35 µg/m^3, despite the consecutive annual decline. Figure 3 shows the spatial distribution of the annual mean PM$_{2.5}$ concentrations in cities throughout China in 2017, assuming that the annual mean PM$_{2.5}$ concentration in a prefecture is represented by the concentrations in the city or cities within
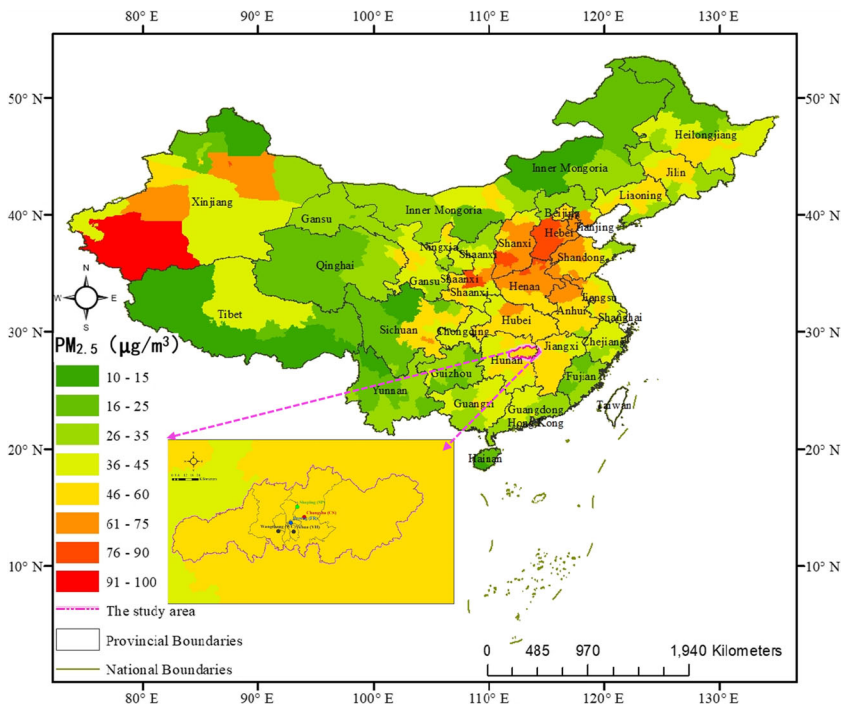

Fig. 3 Spatial distribution of the annual average PM$_{2.5}$ concentrations in Chinese cities in 2017

the prefecture. In terms of the annual average concentration spatial distribution, the worst PM$_{2.5}$ pollution was distributed primarily in BTH and the surrounding areas. The PM$_{2.5}$ concentrations in Changsha were similar to those in BTH and the surrounding areas, which is the most polluted area in central China.

Instrument measurement errors or detection limits include "other" categories required to balance masses. Any underestimation of measured components will also increase the value of the "other" category. The ratio of the "other" category to total PM$_{2.5}$ was much higher in the autumn and winter compared with summer and spring and was higher at the suburban site (SP) than the other sampling sites. Autumn and winter are characterized by a concentration of heavily polluted weather, during which secondary aerosols were relatively high and significantly affected by regional transport. This indicates that the OC and OM concentrations in autumn and winter are possibly underestimated, which would lead to an increase in the relative contribution of the "other" category.

To evaluate the impacts of air mass transport, 48-h back trajectories were calculated using the HYSPLIT model for each season, as illustrated in Fig. 4. Urban PM$_{2.5}$ concentration data were derived from the China National Environmental Monitoring Center (http://www.cnemc.
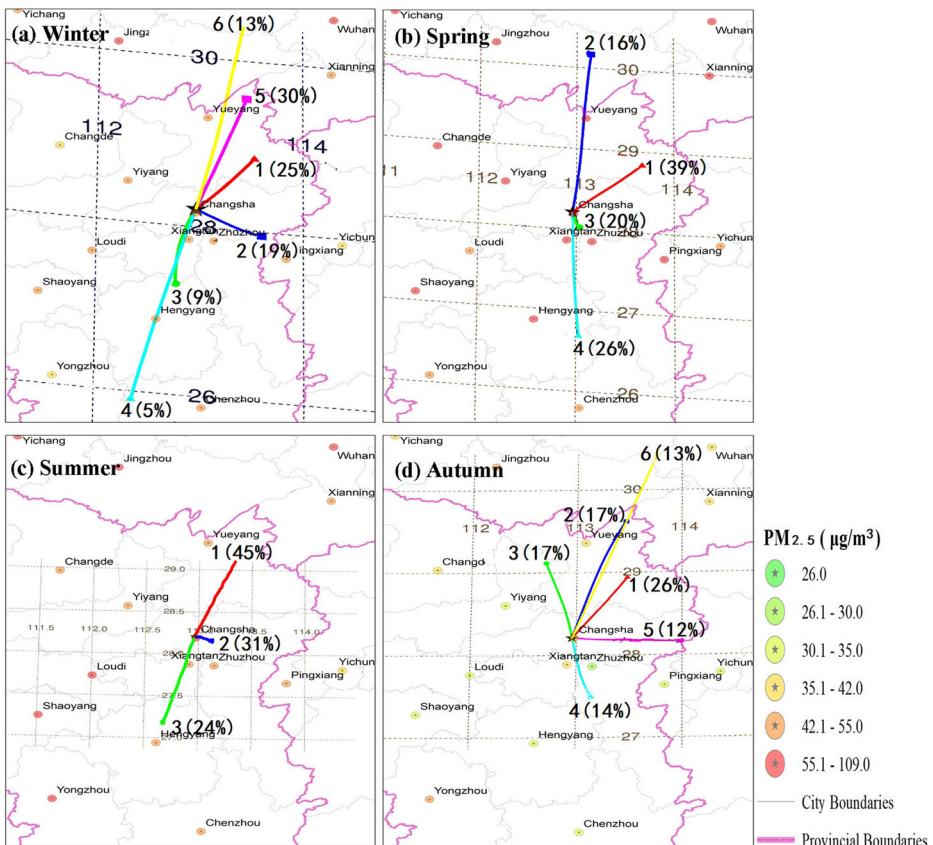
Fig. 4 Forty-eight-hour backward trajectory clusters by season during the PM$_{2.5}$ sampling period. Colored lines and circles represent backward trajectory clusters and average PM$_{2.5}$ concentrations in the trajectory range, respectively

cn/jcbg/kqzlzkbg/) and were used to assess the air pollution status in the backward trajectory range.

In winter, six major air masses contribute to Changsha $PM_{2.5}$ pollution, i.e., those originating from the northeast (air masses 1, 5, and 6), southwest (air masses 3 and 4), and west (air mass 2). A significant north–south transport channel occurs in winter (air masses 4 and 6). Air Mass 6 originates from Wuhan and the surrounding urban clusters and traverses northern Hunan Province, which has the highest concentration of $PM_{2.5}$. The other air masses (1, 2, 3, and 5) all arrive from cities in Hunan Province, which is consistent with the key control regions (CZX Urban Agglomeration).

In spring, four major air masses influence Changsha. Air Mass 2 and 4 are consistent with the north–south transport channels in winter. Air Mass 3 arrives from the south and Air Mass 1 mainly originates from Yueyang. Regional transport of $PM_{2.5}$ has the least effect in the summer, where all three air masses originate from the CZX Urban Agglomeration and surrounding cities, and is essentially not affected by the pollution from outside the province. Six air masses in autumn are approximately similar to those in winter. Air Mass 3, which originates from Changde in the northwest, is characterized by several differences.

In summary, the north–south transport channel was a more important air mass transport trajectory in Changsha, and its contribution to $PM_{2.5}$ pollution was relatively high.

3.2 Spatio-temporal distribution and chemical components of $PM_{2.5}$

Figures 5 and 6 show the spatio-temporal distribution of $PM_{2.5}$ and its chemical components at the five sampling sites. For the five sampling sites, the mean OM accounts for $26.2 \pm 1.0\%$ of the total $PM_{2.5}$ concentration and was the largest contributor to $PM_{2.5}$, ranging from 24.5% (YH) to 27.4% (CS). The second largest fraction was SO_4^{2-}, contributing $21.1 \pm 1.7\%$ of the total $PM_{2.5}$ concentration. Both NO_3^- and NH_4^+ accounted for approximately $18.3 \pm 1.5\%$ and $9.0 \pm 0.8\%$, respectively. At the YH and SP sites, the contribution of EC was 4.3% and 3.2%, respectively. For the annual mean concentration, the elements contributed to $15.0 \pm 4.7\%$ of the $PM_{2.5}$ mass, higher than Lanzhou ($8.8 \pm 2.9\%$) (Wang et al. 2016) and Heze (12.5%) (Liu et al. 2017). The most abundant elements are crustal elements (e.g., Na, Mg, Al, K, Ca and Fe), which account for $74.9 \pm 2.3\%$ of the total analyzed elements, and this percentage was lower
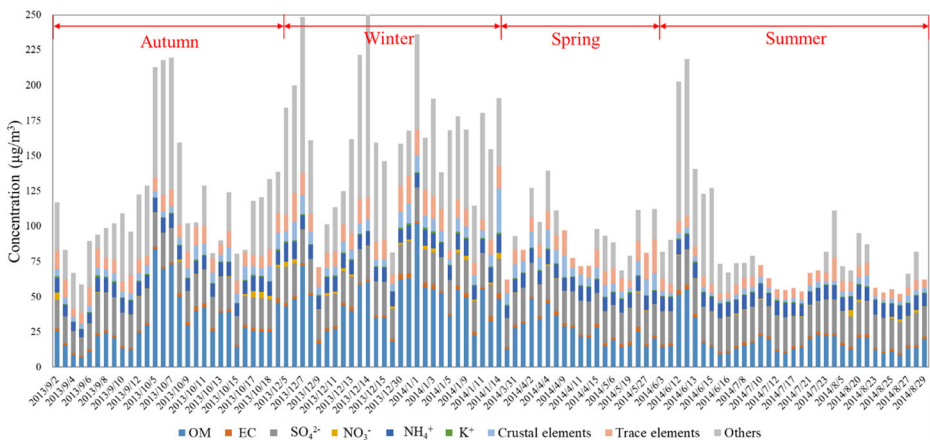
Fig. 5 A time series of total $PM_{2.5}$ and major components
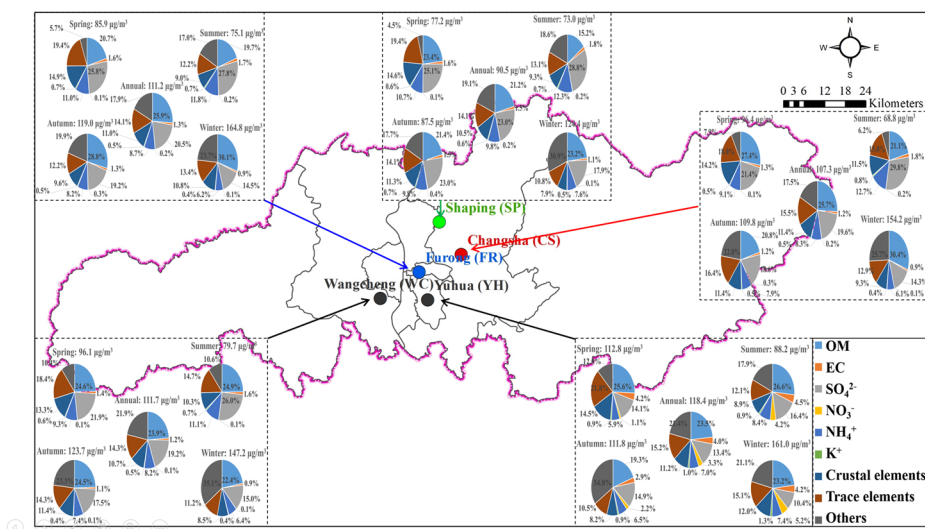
Fig. 6 The variations between the PM$_{2.5}$ chemical components at the five sampling sites

than that found for Lanzhou ($93.6 \pm 4.5\%$) (Wang et al. 2016), and Xinxiang (90.8%) (Feng et al. 2016). The trace elements (V, Cr, Mn, Ni, Cu, Zn, As, Co, Cs, Ag, Cd, P, Ti, and Pb) are present at levels between 33.0 and 56.0 ng m^{-3} and account for $3.8 \pm 1.5\%$ of the PM$_{2.5}$ mass. All five sampling sites showed similar seasonal pollution trends.

Figure 6 indicates that there was a significant spatial variation in the PM$_{2.5}$ concentrations in Changsha. The PM$_{2.5}$ concentration at the YH site was as high as 118.0 ± 46.0 μg/m^3 and the lowest concentration appeared at the SP site, with a concentration of 88.7 ± 37.4 μg/m^3. The difference between the highest and lowest PM$_{2.5}$ concentration was as much as 29.3 μg/m^3, which was nearly one-third of the PM$_{2.5}$ concentration at the suburban site. For all seasons, the PM$_{2.5}$ concentrations at the five sampling sites can be ranked in an identical descending order: urban residential sites > traffic sites > industrial sites > suburban sites. The urban residential areas have both large population and heavy traffic. In contrast, the industrial areas are located at a distance from the urban areas and have an improved atmospheric environmental capacity. The EC ratio of PM$_{2.5}$ at the residential sites was significantly higher than that at the suburban site, which indicates that the primary emissions from residential areas had a significant contribution (Lin et al., 2009), including the combustion engines in automobiles. The OC/EC ratio is a simple method to estimate primary vs. secondary contribution, where ratios exceeding 2 primarily indicate the dominance of a secondary aerosol (Chow et al. 1996). In this study, the mean OC/EC ratio was as high as 7.1, which indicates that there is a possible presence of significant secondary organic carbon. The highest OC/EC ratio (8.2) was located in the suburbs, which is possibly due to the fact that the suburbs are more susceptible to the pollution from the surrounding areas of Changsha.

The PM$_{2.5}$ concentration in Changsha also showed remarkable seasonal variation, which was the highest in the winter and the lowest in the summer, with a difference of 73.3 μg/m^3. The prominent episodes of pollution occurred in the autumn and winter and the pollution levels were often reported as 'heavy' or above. This may be due to the unique horseshoe-shaped topography of Changsha, as shown in Fig. 1, where the "horseshoe mouth" faces northward. This landform produces an airflow convergence zone for the dominate northwest winds that arrive in the winter, which results in the

formation of specific meteorological conditions, such as low wind speed, high humidity, low temperatures, and other conditions characteristic of winter. These factors cause significant regional weather stagnation and poor air self-purification, which are unfavorable for pollutant dispersion, whereas relatively low temperatures are favorable for the production and aggregation of new particulate matter (Zhang et al. 2015).

Yao et al. (2018) investigated atmospheric new particle (NPF) formation from sulfuric acid and amines in Shanghai and found high NPF rates explained by high concentrations of sulfuric acid for sub-3-nm particles and then by added contributions of condensing organic species beyond that size, even under the very high preexisting aerosol loading as condensation sink. It's also noted that climate change may also play an important role in the exacerbated winter haze pollution in East Asia and China in recent years as suggested by previous studies (Zou et al. 2017).

Regional transport may also be an important factor that increases winter air pollution in Changsha. According to the urban air quality monitoring data released by the China National Environmental Monitoring Center (http://www.cnemc.cn/jcbg/kqzlzkbg/), the winter 2013 $PM_{2.5}$ concentration in Wuhan was 163.3 μg/m³, which is significantly higher than that in Changsha (129.7 μg/m³). Changsha has the best seasonal air quality in summer. Dominant winds blow westward from the eastern Chinese coast to Changsha during the summer, carrying a much lower concentration of air pollutants. At the same time, there is an absence of large areas of local pollution (e.g., coal pollution or long-range external dust pollution).

Organic matter had the largest contribution to $PM_{2.5}$ concentration in the summer while both the NO_3^- and NH_4^+ proportions significantly declined due to their transformation to a gas phase at elevated temperatures. The EC fraction in $PM_{2.5}$ maintained a relatively stable level at 4% throughout all seasons, whereas the SO_4^{2-} concentrations showed significant seasonal variation. The SO_4^{2-} proportion of the $PM_{2.5}$ mass concentration was the highest in the summer during all seasons, especially at the industrial site, which accounted for 34.8%. This is due to certain meteorological factors in the summer, such as stronger ultraviolet radiation, which favors photochemical reactions and accelerates the conversion of SO_2 to secondary ions (SO_4^{2-}). There was a higher concentration of NH_4^+ in the spring and summer compared with the autumn and winter, which was possibly due to increased agricultural activity. There were no seasonal or regional differences in the concentrations of crustal and trace metals.

3.3 Aerosol chemistry and ions balance

Understanding the acidity of the aerosol is significantly important due to it being a key parameter that affects heterogeneous reactions, hygroscopic growth, and toxicity of atmospheric aerosol, as well as the neutralizing process of acid rain (Shi et al. 2017a, 2017b; Tao et al. 2013). The molar ratios of cation equivalents (CE) and anion equivalents (AE) are frequently employed to infer the acidity of aerosol (Chow et al. 1994; Hennigan et al. 2015). At this study, ion balance was evaluated using the following equations.

$$AE(\mu eq \cdot m^{-3}) = \frac{c(Cl^-)}{35.5} + \frac{c(NO_3^-)}{62} + \frac{c(SO_4^{2-})}{48} + \frac{c(F^-)}{19} \tag{1}$$

$$CE(\mu eq \cdot m^{-3}) = \frac{c(NH_4^+)}{18} + \frac{c(Mg^{2+})}{12} + \frac{c(K^+)}{39} + \frac{c(Ca^{2+})}{20} + \frac{c(Na^+)}{23} \tag{2}$$

where c represents the concentration of the ion.

As shown in Fig.7 and Table 2, both anions and cations are strongly correlated and the ratios of AE/CE were slightly higher than one, which indicated that the collected PM was slightly acidic in nature. It means the neutralization of sulfate and nitrate in aerosol was not completely achieved at these sites. For ammonium-associated compounds, $(NH_4)_2SO_4$ preferentially forms due to its low volatility. In contrast, NH_4NO_3 is relatively volatile and NH_4Cl has the most volatility. The AE/CE ratios of the $PM_{2.5}$ were similar to those from urban sites in Southern China but higher than certain sites in northern China (Zhou et al. 2016). As shown in Table 2, the AE/CE ratios were 1.59, 1.81, 1.50, and 1.03 in spring, summer, autumn, and winter, respectively, which indicates that the $PM_{2.5}$ was more acidic in spring and summer compared with autumn and winter.

3.4 Potential sources of PM$_{2.5}$

Correlation analysis between ions may reveal the binding mode and homology between WSIs in atmospheric particulate matter (Huang et al. 2014). The SPSS (v. 19.0) software was used to conduct binary correlation analysis and to analyze the possible sources of WSI in $PM_{2.5}$. Table 3 lists the inter-ion correlation coefficient matrix.

As shown in Table 3, the correlation coefficients between SO_4^{2-}, NO_3^-, NH_4^+, K^+, and Na^+ and the total $PM_{2.5}$ concentration were 0.69, 0.69, 0.79, 0.89, and 0.81, respectively. This indicates that these ions significantly affect the variation in $PM_{2.5}$ concentrations in Changsha,
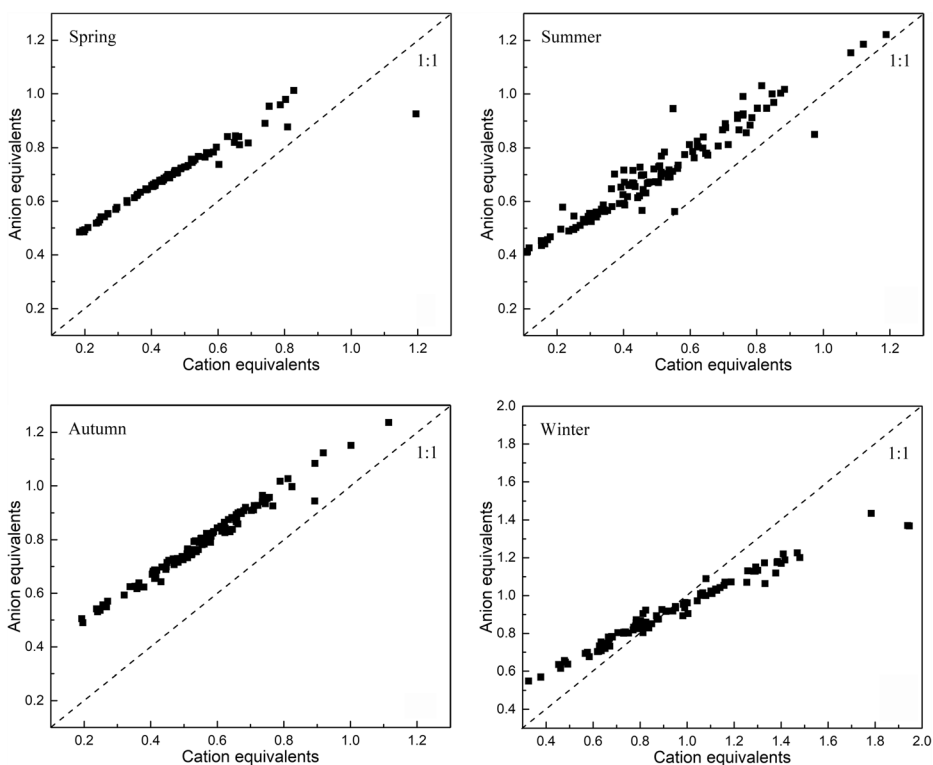

Fig. 7 Correlations between anion equivalents and cation equivalents in different seasons

Table 2 The anion equivalent (AE)/cation equivalent (CE) ratios in the PM$_{2.5}$ samples

Sampling site	Autumn	Winter	Spring	Summer	Annual average
Furong (FR)	1.49	1.00	1.63	1.73	1.46
Changsha (CS)	1.46	1.03	1.69	1.58	1.44
Shaping (SP)	1.59	1.08	1.68	1.47	1.46
Wangcheng (WC)	1.44	1.01	1.45	2.83	1.68
Yuhua (YH)	1.50	1.03	1.50	1.43	1.37
Average	1.50	1.03	1.59	1.81	1.48

which is consistent with the results from Baotou (Zhou et al. 2018) and Jeonju, South Korea (Lee et al. 2001).

The correlation coefficient between Na$^+$ and F$^-$ was as high as 0.72. In the absence of marine sources in Changsha, Na$^+$ can be used to indicate sources from soil dust and coal combustion gases (Osada et al. 2002) while F$^-$ indicates sources from industrial factories, such as aluminum processing and phosphate fertilizer plants (Yang et al. 2009). There was also a high correlation between Na$^+$ and K$^+$, which is possibly due to the fact that these elements exist in atmospheric particulate matter from the source of biomass burning (Liu et al. 2016). There was a relatively high correlation between NO$_3^-$ and NH$_4^+$ (R = 0.78), which indicates that these ions are derived from an identical source, i.e., possibly agricultural fertilizer. The correlation was higher between NH$_4^+$ and SO$_4^{2-}$ (R = 0.81) than NO$_3^-$ and NH$_4^+$ (R = 0.78), which indicates that NH$_4$NO$_3$ is more volatile compared with (NH$_4$)$_2$SO$_4^{2-}$ (He et al. 2012). There was a relatively high correlation between Ca^{2+} and Mg^{2+} (R = 0.60), which suggests that both cations are derived from an identical source, i.e., soil and construction dust.

The relative importance of stationary and mobile sources of N and S emissions to the atmosphere can be determined using the ratios of NO$_3^-$ and SO$_4^{2-}$ in PM$_{2.5}$ (Wang et al. 2005). Previous studies have shown that, when the [NO$_3^-$]/[SO$_4^{2-}$] ratio in PM$_{2.5}$ is greater than 1, the effects of mobile sources (e.g., motor vehicles) are stronger than those of stationary sources (e.g., coal combustion). Otherwise, the effects of stationary sources are stronger than mobile sources (Zhou et al. 2016). Table 4 lists the [NO$_3^-$]/[SO$_4^{2-}$] ratios in the PM$_{2.5}$ samples from the different sampling sites during different seasons. These ratios ranged from 0.67 to 1.07, with an overall average of 0.76 across the five sampling sites in the study area. The [NO$_3^-$]/[SO$_4^{2-}$] ratio exceeded 1 in the winter and remained below 1 during the other seasons, which suggests that stationary sources, during all

Table 3 A correlation analysis of water-soluble ions (WSIs) in PM$_{2.5}$

Component	PM$_{2.5}$	F$^-$	Cl$^-$	NO$_3^-$	SO$_4^{2-}$	K$^+$	Ca^{2+}	Na$^+$	Mg^{2+}	NH$_4^+$
PM$_{2.5}$	1.00	0.65	0.53	0.69**	0.69**	0.89**	0.42	0.81**	0.55	0.79**
F$^-$		1.00	0.55	0.65	0.34	0.66**	0.53	0.72**	0.73**	0.59
Cl$^-$			1.00	0.45	0.21	0.57**	0.58**	0.68**	0.49	0.40
NO$_3^-$				1.00	0.37	0.69	0.31	0.68	0.56	0.78**
SO$_4^{2-}$					1.00	0.62	0.26	0.58	0.24	0.81**
K$^+$						1.00	0.42	0.81**	0.56	0.75**
Ca^{2+}							1.00	0.63**	0.60**	0.31
Na$^+$								1.00	0.76**	0.73**
Mg^{2+}									1.00	0.47
NH$_4^+$										1.00

Note: ** indicates that the correlation is significant at the 0.01 significance level (two-tailed); * indicates that the correlation is significant at the 0.05 significance level (two-tailed)

Table 4 The $[NO_3^-]/[SO_4^{2-}]$ ratios in $PM_{2.5}$ samples between the sampling sites

Sampling sites	Autumn	Winter	Spring	Summer	Annual average
Furong(FR)	0.79	1.01	0.83	0.86	0.79
Changsha(CS)	0.70	1.05	0.84	0.96	0.70
Shaping(SP)	0.67	0.96	0.69	0.79	0.67
Wangcheng(WC)	0.85	1.07	0.84	0.86	0.85
Yuhua(YH)	0.80	1.05	0.74	0.93	0.80
Average	0.76	1.03	0.79	0.88	0.76

seasons except winter, primarily affect the $PM_{2.5}$ in Changsha. During the daytime, photochemical reactions between NO_2 and OH free radicals (Kitto et al., 1992) mainly generate atmospheric HNO_3, followed by the reaction between HNO_3 (g) and NH_3 (g) that forms NH_4NO_3 (s). Since this is an exothermal reaction, lower temperatures and higher humidity favor NH_4NO_3 (s) formation (Zhou et al. 2016). The highest concentrations of nitrate measured in winter are possibly due to sources of local pollution, such as vehicular traffic (Paraskevopoulou et al. 2015), and the $[NO_3^-]/[SO_4^{2-}]$ ratio was the lowest at the SP site, which is due to reduced traffic volume and increased vegetation coverage in suburban areas. Since mobile sources have a greater contribution to atmospheric particulate matter in the winter in Changsha, reducing urban car exhaust emissions is an important step to improve the quality of the atmospheric environment during the high-pollution season (winter). Furthermore, limiting fossil fuel combustion, such as coal, will also help to reduce the concentrations of various water-soluble ions in $PM_{2.5}$ and the overall mass concentration of $PM_{2.5}$.

Table 5 lists the $[NO_3^-]/[SO_4^{2-}]$ ratios in $PM_{2.5}$ samples from typical cities, both local and foreign, reported in recent literature. The average $[NO_3^-]/[SO_4^{2-}]$ ratio of the $PM_{2.5}$ samples from Changsha (0.76) is lower than the ratio in Beijing and other northern cities but higher than that in Guangzhou and similar to the ratio in the Chinese coastal city of Ningbo.

4 Conclusions

This study presented the spatio-temporal variation in $PM_{2.5}$ and its chemical components in Changsha over a 1-year period (September 2013 to August 2014). The mean annual $PM_{2.5}$ concentration was 105.2 ± 11.0 μg/m³, which is significantly higher than other developed

Table 5 A comparison of the $[NO_3^-]/[SO_4^{2-}]$ in $PM_{2.5}$ between Changsha and other cities

City	Period	$[NO_3^-]/[SO_4^{2-}]$
Changsha (the present study)	2013.9–2014.8	0.76
Beijing (Zíková et al. 2016)	2012.6–2013.4	0.96
Shanghai (Huang et al. 2014)	2012.3–2012.5	0.90
Guangzhou (Chen et al. 2017)	2011.12–2012.2	0.39
Nanjing (Wang et al. 2016b)	2013.10–2014.11	0.67
Ningbo, Zhejiang (Li et al. 2017)	2012.12–2013.11	0.79
Yokohama, Japan (Khan et al. 2010)	2007–2008	0.25
Barcelona, Spain (Salameh et al. 2015)	2011.2–2011.12	0.36
Marseilles, France (Salameh et al. 2015)	2011.7–2012.7	0.77
Venice, Italy (Salameh et al. 2015)	2011.1–2011.12	1.59
Thessaloniki, Greece (Salameh et al. 2015)	2011.6–2012.5	0.62

regions (e.g., the YRD and PRD) and is more similar to the most polluted region in China (i.e., the BTH). On average, residential sites had the highest concentrations of $PM_{2.5}$ and chemical species while a suburban site had the lowest concentrations. In general, $PM_{2.5}$ concentrations exhibit noticeable seasonal pollution characteristics in Changsha, with the highest concentrations in the winter and lowest in the summer, with a difference of 73.3 $\mu g/m^3$.

Ion balance calculations show that the $PM_{2.5}$ samples at the five sites were generally acidic, with increased acidity in spring and summer compared with autumn and winter. The AE/CE ratios varied from 1.00 to 2.83, with an average of 1.48 ± 0.40, which is similar to other urban sites in southern China but higher than several sites in northern China. The north–south transport channel is the most significant air mass trajectory. Air masses originating from Wuhan and surrounding urban clusters, as well as from the CZX Urban Agglomeration and surrounding cities, have a significant impact on $PM_{2.5}$ pollution in Changsha.

Compliance with ethical standards

Conflict of interest The authors declare no competing financial interests.

References

Charlson, R.J., Schwartz, S.E., Hales, J.M., Cess, R.D., Coakley JA Jr, Hansen, J.E., Hofmann, D.J.: Climate forcing by anthropogenic aerosols. Science. **255**(5043), 423–430 (1992)

Chen, X.C., Jahn, H.J., Engling, G., et al.: Chemical characterization and sources of personal exposure to fine particulate matter ($PM_{2.5}$) in the megacity of Guangzhou. China Environ Pollut. **231**, 871–881 (2017)

Chow, J.C., Watson, J.G., Fujita, E.M., et al.: Temporal and spatial variations of $PM_{2.5}$ and PM_{10} aerosol in the Southern California air quality study. Atmos. Environ. **28**(12), 2061–2080 (1994)

Chow, J.C., Watson, J.G., Lu, Z., et al.: Descriptive analysis of $PM_{2.5}$ and PM_{10} at regionally representative locations during SJVAQS/AUSPEX. Atmos. Environ. **30**(12), 2079–2112 (1996)

Chow, J.C., Watson, J.G., Edgerton, S.A., Vega, E.: Chemical composition of $PM_{2.5}$ and PM_{10} in Mexico City during winter 1997. Sci. Total Environ. **287**(3), 177–201 (2002)

Draxler, R.R., Hess, G.D.: An overview of the HYSPLIT 4 modelling system for trajectories, dispersion, and deposition. Aust. Meteorol. Mag. **47**, 295–308 (1998)

Feng, J., Yu, H., Su, X., et al.: Chemical composition and source apportionment of $PM_{2.5}$ during Chinese spring festival at Xinxiang, a heavily polluted city in North China: fireworks and health risks. Atmos. Res. **182**, 176–188 (2016)

Guan, Y., Kang, L., Wang, Y., et al.: Health loss attributed to $PM_{2.5}$ pollution in China's cities: economic impact, annual change and reduction potential. J. Clean. Prod. **217**, 284–294 (2019)

Guo, S., Hu, M., Wang, Z.B., et al.: Size-resolved aerosol water-soluble ionic compositions in the summer of Beijing: implication of regional secondary formation. Atmos. Chem. Phys. **10**(6), 947–959 (2009)

Haywood, J.M., Ramaswamy, V.: Global sensitivity studies of the direct radiative forcing due to anthropogenic sulfate and black carbon aerosols. J. Geophys. Res. Atmos. **103**(D6), 6043–6058 (1998)

He, K., Zhao, Q., Ma, Y., et al.: Spatial and seasonal variability of $PM_{2.5}$ acidity at two Chinese megacities: insights into the formation of secondary inorganic aerosols. Atmos. Chem. Phys. Discuss. **12**, 25557–25603 (2012)

Hennigan, C.J., Izumi, J., Sullivan, A.P., et al.: A critical evaluation of proxy methods used to estimate the acidity of atmospheric particles. Atmos. Chem. Phys. **15**, 2775–2790 (2015)

Huang, G., Cheng, T., Zhang, R., et al.: Optical properties and chemical composition of $PM_{2.5}$ in Shanghai in the spring of 2012. Particuology. **13**, 52–59 (2014)

Khan, M.F., Shirasuna, Y., Hirano, K., Masunaga, S.: Characterization of $PM_{2.5}$, $PM_{2.5-10}$ and $PM_{>10}$ in ambient air, Yokohama, Japan. Atmos. Res. **96**(1), 159–172 (2010)

Kitto AMN, Harrison RM. Nitrous and nitric acid measurement at site in south-east England, Atmos Environ 26: 235-241 (1992)

Lee HS, Wang BW, Chemical characteristics of principal PM2.5 species in Chongju, South Korea, Atmos Environ 35(4):739-746 (2001)

Li, M., Hu, M., Du, B., et al.: Temporal and spatial distribution of $PM_{2.5}$ chemical composition in a coastal city of Southeast China. Sci. Total Environ. **605**, 337–346 (2017)

Lim, H.J., Turpin, B.J.: Origins of primary and secondary organic aerosol in Atlanta: results of time-resolved measurements during the Atlanta supersite experiment. Environ Sci Technol. **36**(21), 4489–4496 (2002)

Lin P, Hu M, Deng Z, et al., Seasonal and diurnal variations of organic carbon in PM2.5 in Beijing and the estimation of secondary organic carbon, J Geophys Res-Atmos 114 (D2) (2009)

Liu, L., Wang, Y.L., Du, S.Y., et al.: Single particle analysis during heavy air pollution episodes in January 2014 in Beijing. Acta Sci. Circumst. **34**(2), 630–637 (2016) (In Chinese)

Liu, B., Wu, J., Zhang, J., Wang, L., Yang, J., Liang, D., Dai, Q., Bi, X., Feng, Y., Zhang, Y., Zhang, Q.: Characterization and source apportionment of $PM_{2.5}$ based on error estimation from EPA PMF 5.0 model at a medium city in China. Environ. Pollut. **222**, 10–22 (2017)

Ma, Q., Wu, Y., Zhang, D., et al.: Roles of regional transport and heterogeneous reactions in the $PM_{2.5}$ increase during winter haze episodes in Beijing. Sci. Total Environ. **599**, 246–253 (2017)

MEP: The Twelfth Five-Year Plan for Prevention and Control of Atmospheric Pollution in Key Regions. Ministry of Environmental Protection of the People's Republic of China (2012) (in Chinese). http://www.zhb.gov.cn/gkml/hbb/bwj/201212/t20121205_243271.htm

Osada, K., Kido, M., Nishita, C., et al.: Changes in ionic constituents of free tropospheric aerosol particles obtained at Mt. Norikura (2770 m asl), Central Japan, during the Shurin period in 2000. Atmos. Environ. **36**(35), 5469–5477 (2002)

Paraskevopoulou, D., Liakakou, E., Gerasopoulos, E., et al.: Sources of atmospheric aerosol from long-term measurements (5 years) of chemical composition in Athens, Greece. Sci. Total Environ. **527**, 165–178 (2015)

Qiu, X., Duan, L., Gao, J., Wang, S.L., et al.: Chemical composition and source apportionment of PM_{10} and $PM_{2.5}$ in different functional areas of Lanzhou, China. J. Environ. Sci. **40**, 75–83 (2016)

Salameh, D., Detournay, A., Pey, J., et al.: $PM_{2.5}$ chemical composition in five European Mediterranean cities: a 1-year study. Atmos. Res. **155**, 102–117 (2015)

Shi, Z., Li, J., Huang, L., et al.: Source apportionment of fine particulate matter in China in 2013 using a source-oriented chemical transport model. Sci. Total Environ. **601**, 1476–1487 (2017a)

Shi, G., Xu, J., Peng, X., Xiao, Z., Chen, K., Tian, Y., Guan, X., Feng, Y., Yu, H., Nenes, A., Russell, A.G.: pH of aerosols in a polluted atmosphere: source contributions to highly acidic aerosol. Environ Sci Technol. **51**(8), 4289–4296 (2017b)

Tao, J., Zhang, L., Engling, G., et al.: Chemical composition of $PM_{2.5}$ in an urban environment in Chengdu, China: importance of springtime dust storms and biomass burning. Atmos. Res. **122**, 270–283 (2013)

Wang, G., Huang, L., Gao, S., et al.: Characterization of water-soluble species of PM_{10} and $PM_{2.5}$ aerosols in urban area in Nanjing, China. Atmos. Environ. **36**(8), 1299–1307 (2002)

Wang, Y., Zhuang, G., Tang, A., et al.: The ion chemistry and the source of $PM_{2.5}$ aerosol in Beijing. Atmos. Environ. **39**(21), 3771–3784 (2005)

Wang, X.M., Hua, T., Zhang, C.X., et al.: Aeolian salts in Gobi deserts of the western region of Inner Mongolia: gone with the dust aerosols. Atmos. Res. **118**, 1–9 (2012)

Wang, H., Zhu, B., Shen, L., et al.: Water-soluble ions in atmospheric aerosols measured in five sites in the Yangtze River Delta, China: size-fractionated, seasonal variations and sources. Atmos. Environ. **123**, 370–379 (2015)

Wang, Y., Jia, C., Tao, J., Zhang, L., Liang, X., Ma, J., Gao, H., Huang, T., Zhang, K.: Chemical characterization and source apportionment of $PM_{2.5}$ in a semi-arid and petrochemical-industrialized city, Northwest China. Sci. Total Environ. **573**, 1031–1040 (2016)

Wang, H.L., Qiao, L.P., Lou, S.R., et al.: Chemical composition of $PM_{2.5}$ and meteorological impact among three years in urban Shanghai, China. J. Clean. Prod. **112**, 1302–1311 (2016a)

Wang, H., An, J., Cheng, M., et al.: One year online measurements of water-soluble ions at the industrially polluted town of Nanjing, China: sources, seasonal and diurnal variations. Chemosphere. **148**, 526–536 (2016b)

Watson, J.G., Chow, J.C., Chen, L.W.: Summary of organic and elemental carbon/black carbon analysis methods and Intercomparisons. Aerosol Air Qual. Res. **5**, 65–102 (2005)

White, W.H., Roberts, P.T.: On the nature and origins of visibility-reducing aerosols in the Los Angeles air basin. Atmos. Environ. **11**(9), 803–812 (1997)

Yan, D., Lei, Y., Shi, Y., et al.: Evolution of the spatiotemporal pattern of $PM_{2.5}$ concentrations in China–a case study from the Beijing-Tianjin-Hebei region. Atmos. Environ. **183**, 225–233 (2018)

Yang, X.Y., Yamada, M., Tang, N., Lin, J.M., Wang, W., Kameda, T., Toriba, A., Hayakawa, K.: Long-range transport of fluoride in East Asia monitored at Noto peninsula, Japan. Sci. Total Environ. **407**(16), 4681–4686 (2009)

Yao, L., Garmash, O., Bianchi, F., et al.: Atmospheric new particle formation from sulfuric acid and amines in a Chinese megacity. Science. **361**(6399), 278–281 (2018)

Zhang, P., Wu, J.N.: Impact of mandatory targets on $PM_{2.5}$ concentration control in Chinese cities. J. Clean. Prod. **197**, 323–331 (2018)

Zhang, C., Ni, Z., Ni, L.: Multifractal detrended cross-correlation analysis between $PM_{2.5}$ and meteorological factors. Phys A. **438**, 114–123 (2015)

Zhang, Q., Jiang, X., Tong, D., Davis, S.J., Zhao, H., Geng, G., Feng, T., Zheng, B., Lu, Z., Streets, D.G., Ni, R., Brauer, M., van Donkelaar, A., Martin, R.V., Huo, H., Liu, Z., Pan, D., Kan, H., Yan, Y., Lin, J., He, K., Guan, D.: Transboundary health impacts of transported global air pollution and international trade. Nature. **543**(7647), 705–709 (2017a)

Zhang, Z., Wang, W., Cheng, M., et al.: The contribution of residential coal combustion to $PM_{2.5}$ pollution over China's Beijing-Tianjin-Hebei region in winter. Atmos. Environ. **159**, 147–161 (2017b)

Zhang, N.N., Ma, F., Qin, C.B., Li, Y.F.: Spatiotemporal trends in $PM_{2.5}$ levels from 2013 to 2017 and regional demarcations for joint prevention and control of atmospheric pollution in China. Chemosphere. **210**, 1176–1184 (2018a)

Zhang, Y., Lang, J., Cheng, S., Li, S., Zhou, Y., Chen, D., Zhang, H., Wang, H.: Chemical composition and sources of PM 1 and $PM_{2.5}$ in Beijing in autumn. Sci. Total Environ. **630**, 72–82 (2018b)

Zhang, W., Wang, F., Hubacek, K., et al.: Unequal exchange of air pollution and economic benefits embodied in China's exports. Environ Sci Technol. **52**(7), 3888–3898 (2018c)

Zheng, Y., Zhang, Q., Liu, Y., et al.: Estimating ground-level $PM_{2.5}$ concentrations over three megalopolises in China using satellite-derived aerosol optical depth measurements. Atmos. Environ. **124**, 232–242 (2016)

Zhou, J., Xing, Z., Deng, J., et al.: Characterizing and sourcing ambient $PM_{2.5}$ over key emission regions in China I: water-soluble ions and carbonaceous fractions. Atmos. Environ. **135**, 20–30 (2016)

Zhou, H., Lü, C., He, J., et al.: Stoichiometry of water-soluble ions in $PM_{2.5}$: application in source apportionment for a typical industrial city in semi-arid region, Northwest China. Atmos. Res. **204**, 149–160 (2018)

Zíková, N., Wang, Y., Yang, F., et al.: On the source contribution to Beijing $PM_{2.5}$ concentrations. Atmos. Environ. **134**, 84–95 (2016)

Zou, Y., Wang, Y., Zhang, Y., et al.: Arctic Sea ice, Eurasia snow, and extreme winter haze in China. Sci. Adv. **3**(3), e1602751 (2017)